Project No. 037005

CECILIA

Central and Eastern Europe Climate Change Impact and Vulnerability Assessment

Specific targeted research project

1.1.6.3.I.3.2: Climate change impacts in central-eastern Europe

D3.5: Climate change scenarios for end of century (time slice 2070-2100)

Due date of deliverable: 1st June 2009
Actual submission date: 31st June 2009

Start date of project: 1st June 2006 Duration: 36 months

Lead contractor for this deliverable: Eötvös Loránd University (ELU)

Project co-funded by the European Commission within the Sixth Framework Programme (2002-2006)		
Dissemination Level		
PU	Public	X
PP	Restricted to other programme participants (including the Commission Services)	
RE	Restricted to a group specified by the consortium (including the Commission Services)	
CO	Confidential, only for members of the consortium (including the Commission Services)	

Contributing partners: CUNI, IAP, NMA, ELU

Participant ID Responsible person	SDS methodology	SDS input	SDS output: parameter, grid or stations	SDS domain
CUNI **Jiri Miksovsky**	Dynamical-empirical	ECHAM-RegCM	T_{max}, T_{min}, precipitation (daily); 832 grid points	CECILIA common domain
IAP **Martin Dubrovsky**	Stochastic weather generator (i) Delta approach and (ii) Pattern scaling	11 GCMs from MAGICC	Monthly temperature and precipitation total (Prague)	1 station: Prague
NMA **Aristita Busuioc**	Statistical-based on CCA	8 ENSEMBLES -GCMs (stream1), +ARPEGE	Monthly temperature (94 stations) and precipitation total (16 stations)	LON:20-30°E, LAT:43-50°N (temperature), LON:24-27°E LAT:43-45°N (precipitation)
ELU **Judit Bartholy**	Stochasical	AT-700 hPa (2,5°)	Temperature, precipitation (1° resolution grid)	LON: 16-23°E LAT: 46-49°N

1. Contribution of CUNI

Introduction

Charles University's (CUNI's) contribution to the provision of climate change scenarios is based on the analysis of the outputs of the RegCM3 model, developed at the Abdus Salam International Centre for Theoretical Physics and run at CUNI. A description of the model and its integration domain is provided in the CECILIA deliverable D2.1; basic validation of the run driven by the ECHAM5 GCM, as well as simulated changes in mean temperature and precipitation for the periods 2021-2050 and 2071-2100, are presented in deliverable D2.6.

Along with scenarios based on raw outputs of the RegCM model, series subjected to postprocessing procedure, correcting for systematic errors in the statistical distribution of the target variables, were also used (these are referred to as postprocessed series in the following text). The corrective algorithm applied was based on the modified method of Piani et al. (2009); specific details are given in deliverable D3.2. The validation was carried out for the CECILIA common domain, covering parts of Austria, Czech Republic, Hungary and Slovakia – see deliverable D3.1 for specification of the domain and procedures used to generate the respective gridded datasets of observed values. The outputs of the RegCM model, both original and postprocessed, were IDW-interpolated onto the grid used by the set of observations in the CECILIA common domain.

The selected illustrative results here are presenting absolute or relative differences between the statistics of interest in the simulated climate for the period 2071-2100 and for the control period 1961-1990 (former minus/divided by the latter). For analogical analysis concerning expected changes in the period 2021-2050, see deliverable D3.4.

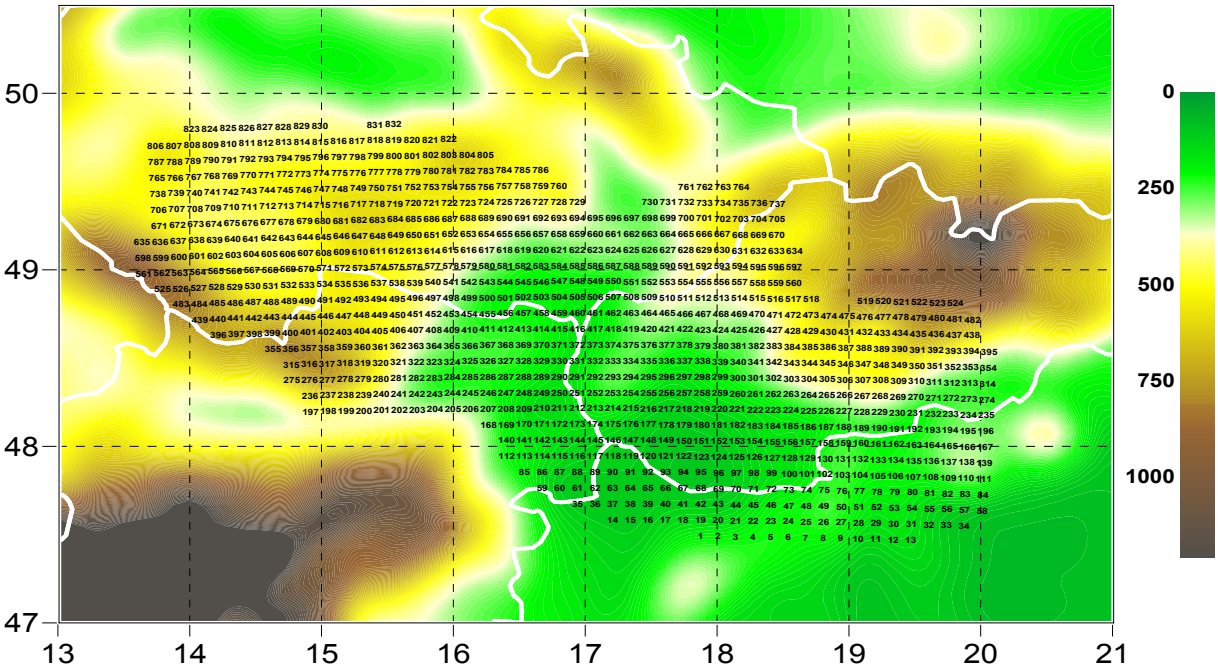

Fig. 1.1: Grid points of CECILIA common validation domain (identification numbers located over the respective gridboxes), drawn over the orography of the RegCM model (m)

The results are presented either in a form of maps covering the entire region of Central Europe (raw model outputs only) or graphs presenting the values of the analysed statistics for individual grid points of the validation domain shown in Fig. 1.1 (postprocessed data are shown along with their equivalents for unprocessed outputs of the RegCM model, to demonstrate the eventual contrast between the two). For analogical results derived for the period 2021-2050, see deliverable D3.4.

Changes of mean values

For the period 2071-2100, slight increase of precipitation is projected for most of the CE region (Fig. 1.2, left). Seasonally, the increase is strongest during the climatic winter and autumn, slight decrease was found for summer,

though it does not appear for all locations (Fig. 1.3). Postprocessed series typically show even higher values of the increase, reaching 50% in some grid points and seasons.

Increase of mean temperature close to 3 °C was typical for most of central Europe (Fig. 1.2, right); similar values of the rise were detected for maximum and minimum temperature as well. The influence of postprocessing on temperature characteristics is distinct and there is a tendency for systematic increase of the climate signal, stronger for maximum temperature than for minimum one (Fig. 1.4). Similarly to the situation for the period 2021-2050, postprocessing brings increased spatial variability of the temperature increase, as well as of precipitation changes.

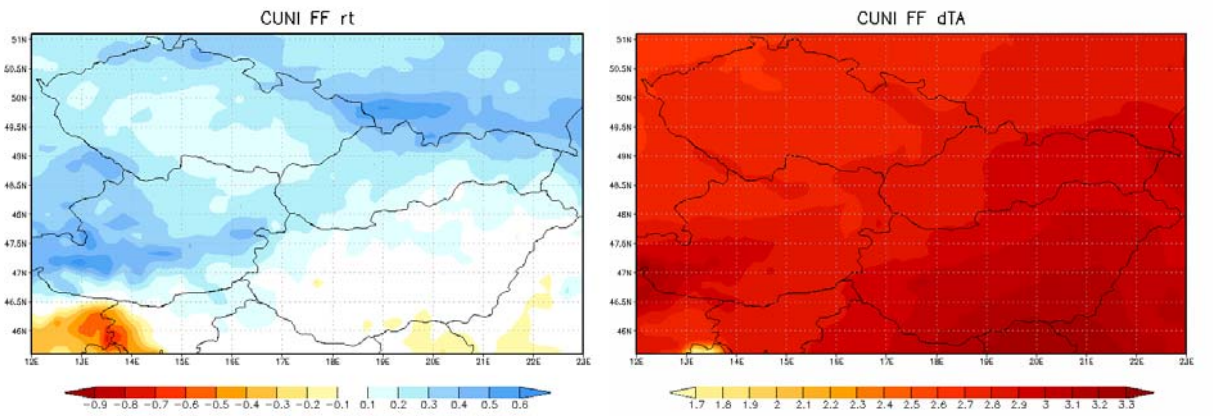

Fig. 1.2: Absolute changes of precipitation (left, mm/day) and mean temperature (right, °C) in the CE region, for the period 2021-2050 relative to 1961-1990 (entire year)

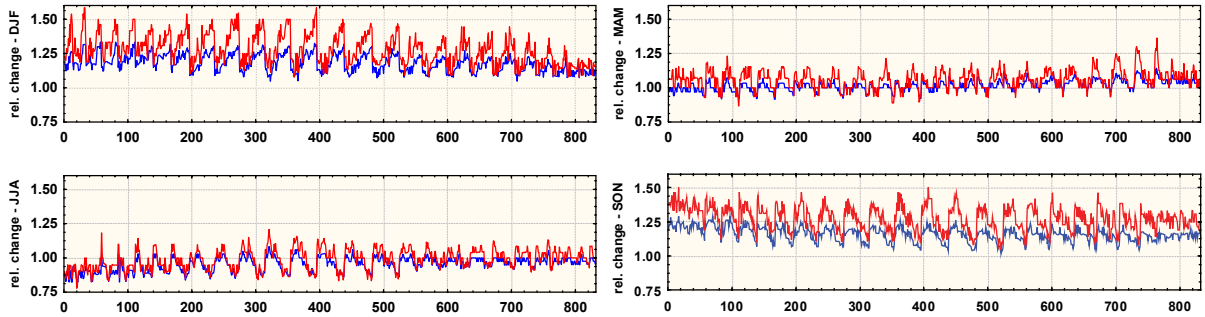

Fig. 1.3: Precipitation change in different seasons, and the influence of postprocessing, for the period 2071-2100 relative to 1961-1990. Blue graph represents change in the original data, red in the postprocessed series; the horizontal axis shows identification numbers of the grid points in the validation domain.

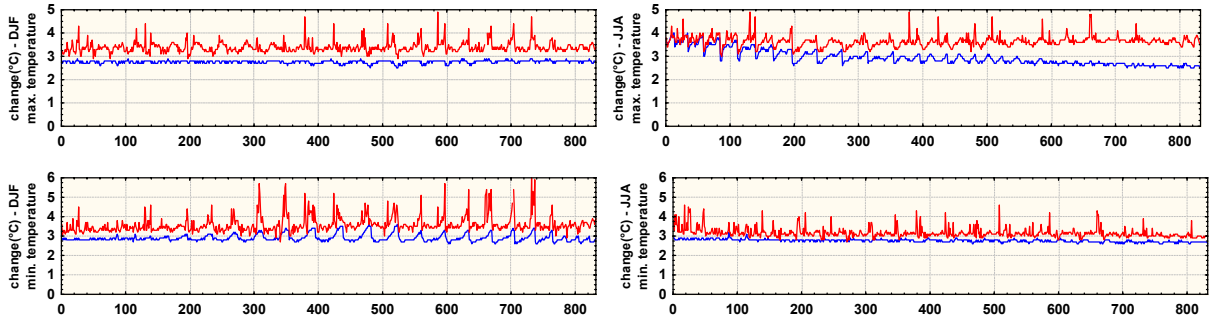

Fig. 1.4: Maximum (top) and minimum (bottom) temperature change in DJF (left) and JJA (right) seasons, and the influence of postprocessing, for the period 2071-2100 relative to 1961-1990. Blue graph represents change in the original data, red in the postprocessed series; the horizontal axis shows identification numbers of the grid points in the validation domain.

Changes in the spread of values

A clear rise of daily precipitation variance is apparent, especially for seasons with mean precipitation increase; for the DJF season, this is shown in Fig. 1.5. A slight amplification of the change appears after the postprocessing

procedure is applied. For temperature characteristics, the variance change is less pronounced in terms of magnitude, and more seasonally diverse.

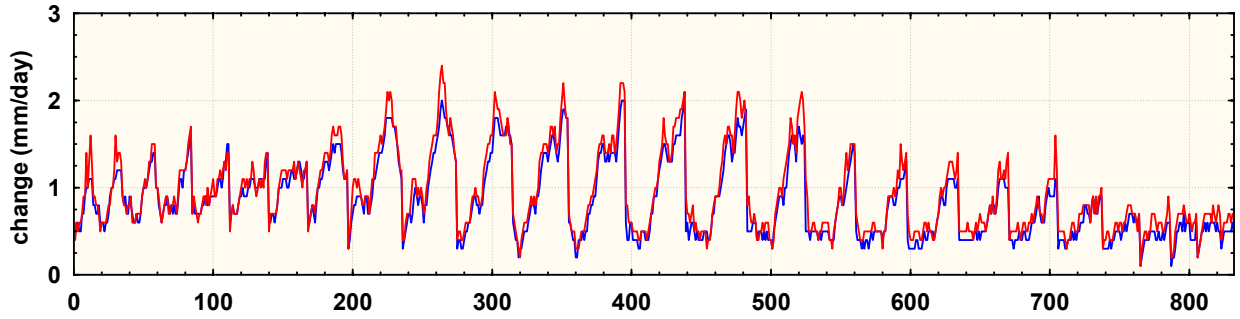

Fig. 1.5: Change of standard deviation of daily precipitation sums in the DJF season, and the influence of postprocessing. Blue graph represents change in the original data, red in the postprocessed series; the horizontal axis shows identification numbers of the grid points in the validation domain.

Changes in the extreme tails of the statistical distributions

The changes of the values of the highest or lowest quantiles of daily temperature or precipitation do not precisely follow the evolution of mean values. In Figs. 1.6, 1.7 and 1.8, this is shown on selected examples, along with the effects of postprocessing. Similarly to the period 2021-2050, there is especially strong increase for the 1% quantile of minimum daily temperature in winter (Fig. 1.7), far exceeding the rise of its mean value and further amplified by postprocessing.

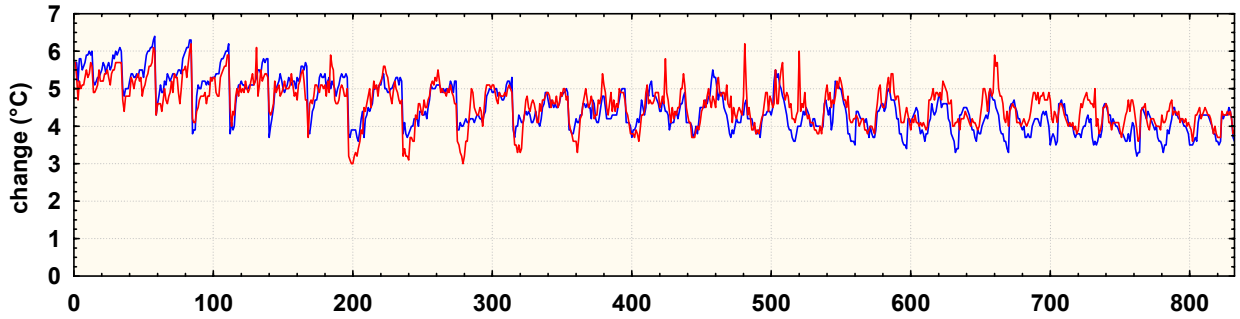

Fig. 1.6: Changes of the value of the 99% quantile of maximum daily temperature, JJA season. Blue graph represents change in the original data, red in the postprocessed series; the horizontal axis shows identification numbers of the grid points in the validation domain.

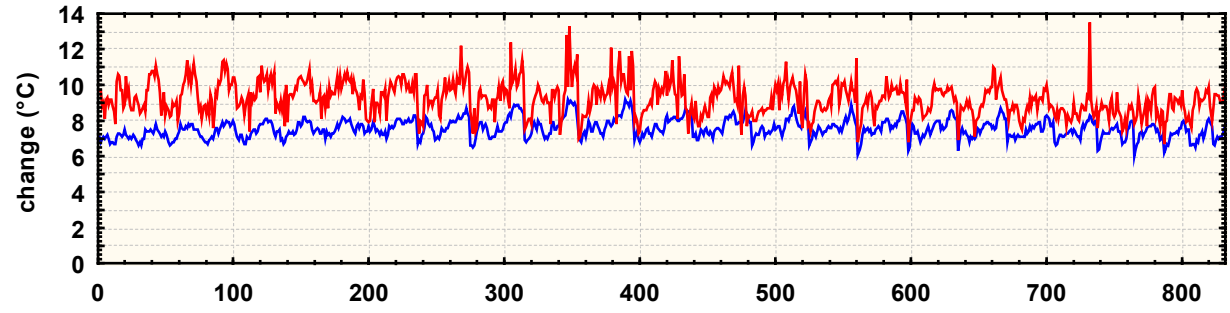

Fig. 1.7: Changes of the value of the 1% quantile of minimum daily temperature, DJF season. Blue graph represents change in the original data, red in the postprocessed series; the horizontal axis shows identification numbers of the grid points in the validation domain.

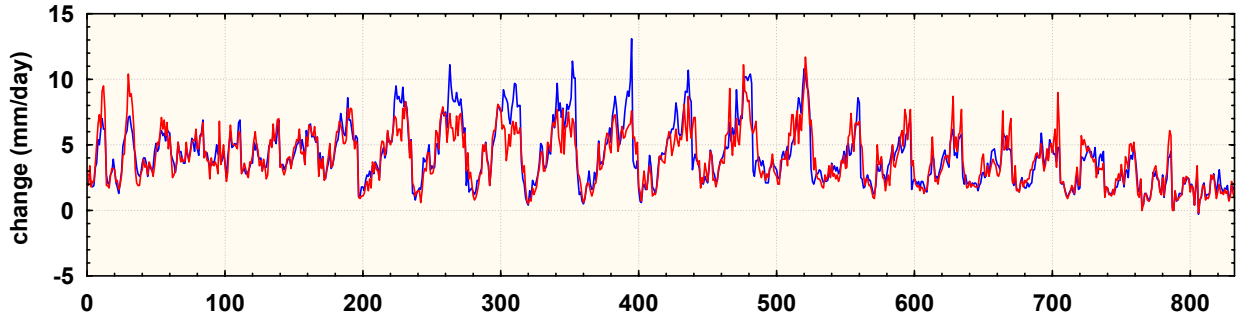

Fig. 1.8: Changes of the value of the 99% quantile of daily precipitation, DJF season. Blue graph represents change in the original data, red in the postprocessed series; the horizontal axis shows identification numbers of the grid points in the validation domain.

Changes of special derived characteristics

Influence of the simulated climate changes on selected characteristics related to the rate of (non)exceedance of characteristic values of temperature or precipitation is shown for a few selected examples in this section. There seems to be a mild tendency towards increase of heavy precipitation events in summer (Fig. 1.9), especially for the northern portion of the validation domain. Very clear is the increase of the number of tropical days (maximum temperature over 30°C), shown in Fig. 1.10; note the profound difference between the results from original model outputs and from the postprocessed series, caused by strong cold bias of the RegCM model. Another distinct effect of the simulated climate change is the drop of the number of days when temperature does fall under the freezing point (Fig. 1.11); in this case, postprocessing does not cause any significant changes of the detected signal.

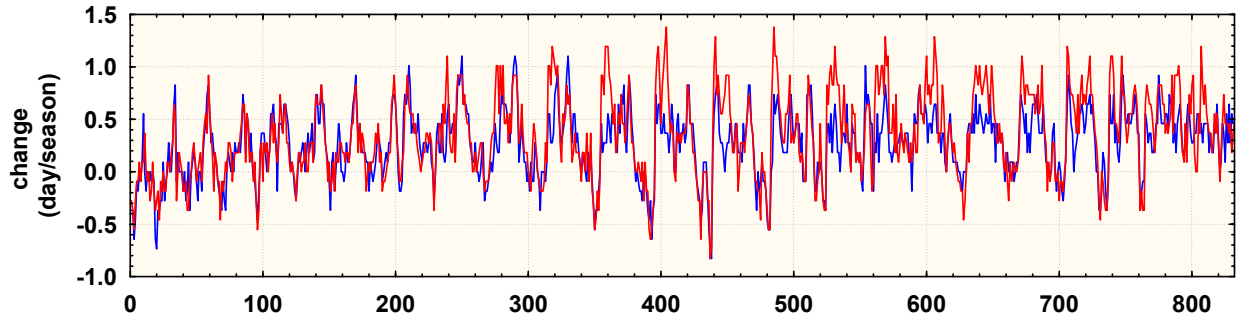

Fig. 1.9: Change of the number of days with precipitation over 20 mm in JJA season. Blue graph represents change in the original data, red in the postprocessed series; the horizontal axis shows identification numbers of the grid points in the validation domain.

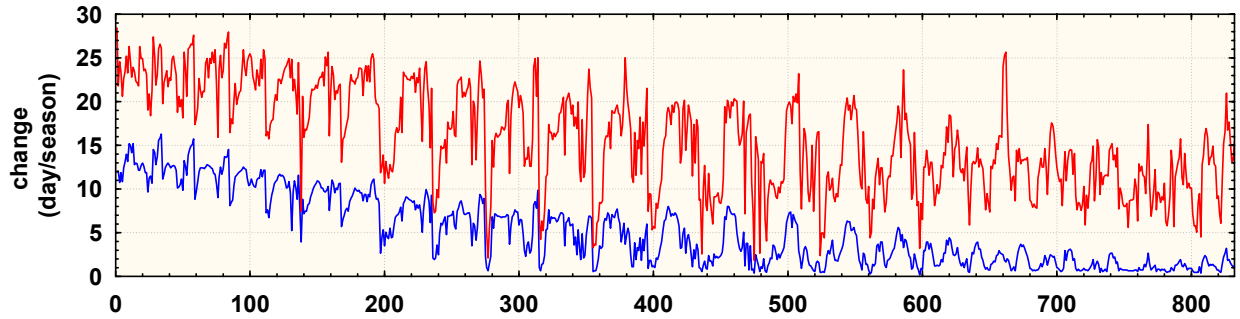

Fig. 1.10: Change of the number of days with maximum daily temperature over 30 °C in JJA season. Blue graph represents change in the original data, red in the postprocessed series; the horizontal axis shows identification numbers of the gridpoints in the validation domain.

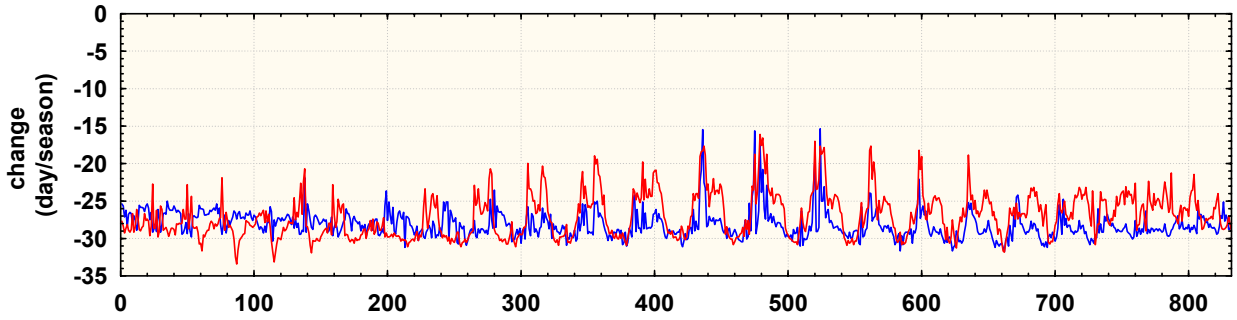

Fig. 1.11: Change of the number of days with minimum temperature below 0 °C in DJF season. Blue graph represents change in the original data, red in the postprocessed series; the horizontal axis shows identification numbers of the grid points in the validation domain.

References:

Piani, C., Haerter, J.O., Coppola, E. (2009): Statistical bias correction for daily precipitation in regional climate models over Europe. Theor Appl Climatol, in print

2. Contribution of IAP

2.1 Introduction

The input weather series for agricultural and hydrological climate change impact experiments in Czechia were mostly prepared by the stochastic weather generator Met&Roll (Dubrovský et al., 2000; Dubrovský et al., 2004), whose parameters were modified according to the climate change scenarios derived from GCM simulations. Two approaches were used to derive the climate change scenarios from the GCM simulations: Delta approach and the Pattern scaling. In the Delta approach, the scenario for a specific future is derived by comparing statistics for the future with respect to those related to the presence (reference period). This approach was used to derive the scenarios from the daily weather series, which are available only for shorter time slices. The pattern scaling method, which is a more preferred method, was used when the scenarios were derived from the monthly GCM output, which is available for much longer periods compared to the dily outputs. The scenarios derived in the Delta approach are loaded by higher sampling error, however they may include also changes in the daily variability.

2.2 Scenarios derived by the pattern scaling method from the monthly GCM outputs

The "Pattern Scaling" method (Dubrovsky et al., 2005) is based on an assumption that the change of each climatic characteristic ΔX is linearly proportional to the change in global mean temperature ΔT_G:

$$\Delta X = \Delta X^* \times \Delta T_G$$

where ΔX^* is the standardised change of X related to 1 degree rise in global mean temperature. The set of standardised changes of all relevant climatic characteristics and for all month is then called the standardised climate change scenario. In our case, the relevant climatic characteristics are: daily average and extreme temperatures, daily precipitation sum and daily global solar radiation. Humidity and wind speed, which are also needed for some impact models, are added by the resampling method because of the incompleteness of the GCM databases. The scenarios derived from the monthly GCM outputs include changes in the means and standard deviations of monthly values of individual climatic characteristics. The changes in temperature means are given in terms of Celsius degrees, changes in all other climatic characteristics (including standard deviations of monthly temperatures) are given in terms of percentage.

Advantages of the pattern scaling method include: (i) the standardised scenarios may be derived (using the linear regression) from a long GCM-simulated time slice (e.g. 1961-2100) which implies a lower sampling error and thereby higher robustness of the scenarios (compared to the Delta approach commonly applied to shorter time slices). (ii) The change in global mean temperature, ΔT_G, which is used to scale the standardised scenarios may be estimated by a simpler (compared to GCM) one-dimensional energy-balance model MAGICC (Harvey et al. 1997, Hulme et al. 2000; http://www.cgd.ucar.edu/cas/wigley/magicc/), which models evolution of the global temperature

in response to chosen emission scenario, climate sensitivity and several other model parameters. This approach allows scaling of the standardised scenarios derived from GCMs run at a single emission scenario for a set of user-selected combinations of emission scenario and climate sensitivity. In result, by using a set of standardised scenarios derived from several GCMs scaled by a suitably selected set of values of the scaling factor (ΔT_G), the pattern scaling method allows to effectively account for uncertainties in these two major driving constraints. The use of the pattern scaling method thus allows to bypass the two shortcomings of the available set of GCM simulations: (i) The outputs from existing GCM simulations (Fig.2.1) show, that the ΔT_G projections till 2100 based on available GCM set do not account for the uncertainty in climate sensitivity (which is a topic of broad scientific discussions). (ii) The GCM database does not include all 4 markers emission scenarios in individual GCMs.

Construction of the standardised scenarios: The standardised scenarios are derived from the GCM-simulated time series of monthly averages of climatic characteristics using a linear regression, in which the global mean temperature is the independent variable, and the respective climatic characteristic is a dependent variable. The standardised scenarios for the CECILIA project were derived from the most recent GCM simulations (SRES-A2 emission scenario) made for the IPCC 4th Assessment Report (IPCC, 2007). Specifically, SRES-A2 runs were used. This emission scenario assumes the highest GHG emissions of the four marker emission scenarios, so that it implies highest signal-to-noise ratio and thereby the lowest error in estimating the standardised scenario. The resultant standardised scenario may be scaled for more "optimistic" emission scenarios (= lower emissions scenarios); the scaling for more pessimistic emission scenarios (= higher emissions scenarios) than those used for estimating the standardised scenario is not recommended: this would imply extrapolation, which is loaded by much higher error.

Choice of the GCMs: Figure 2.2 shows the standardised scenarios for temperature and precipitation for 11 GCMs. The differences between scenarios derived from individual GCMs are due to differences in the GCMs (related to different parameterization of sub-grid phenomena, different spatial resolution, different representations of Earth surface, …) and natural climate variability (the latter may be effectively modelled by the stochastic weather generator, which is linked to the climate change scenarios). To account for the inter-GCM variability in the given climate change impact analysis, we can either use scenarios from all available GCMs, or to use a subset of GCMs which consists of those GCMs which are among the best (in terms of the fit between observed climate and GCM-simulated climate) and represent the between model variability. Considering the amount of GCMs, we used a latter approach. Based on the earlier validation tests (Dubrovsky et al. 2005) the triplet of GCMs was used to define the standardised scenarios: HadCM3, ECHAM5 and NCAR-PCM, which satisfy the above conditions (simultaneously, the benefit of this triplet is that the chosen GCMs belong to the most frequently worldwide used GCMs, which allows comparison of results obtained with these scenarios with results of other authors.

Choice of the values of the scaling factor, ΔT_G: The increase in global mean temperature ΔT_G was estimated by one-dimensional energy-balance model MAGICC. To account for the uncertainties in climate sensitivity and emission scenarios, all possible combinations of the four marker emission scenarios (SRES-A1, SRES-A2, SRES-B1 and SRES-B2) and three values of climate sensitivity (low = 1.5 K, middle = 2.6 K, high = 4.5 K) were used to drive MAGICC while estimating the value of ΔT_G. Of the 12 resultant values, we used three (found in the bottom line of the table): the LOW (highlighted in yellow colour) is the lowest of the four values related to the low climate sensitivity and 4 emission scenarios, the MIDDLE (highlighted in blue) is the median of the four values related to the middle climate sensitivity, and the HIGH (highlighted in green) is the highest of the four values related to the high climate sensitivity.

Tab.2.1 The increase in global mean temperature (with respect to 1961-1990) for three values of climate sensitivity (low/mid/high: 1.5, 2.6, 4.5 K), four marker emission scenarios (SRES-A1, -A2, -B1, -B2), and three futures (2025, 2050, 2100). The low (optimistic), middle and high (= pessimistic) estimates of ΔT_G are given in the bottom row of the table (SUM).

	2025	2050	2100
	low / mid / high	low / mid / high	low / mid / high
SRES-A1	0.60 / 0.85 / 1.17	1.02 / 1.47 / 2.07	1.49 / 2.21 / 3.24
SRES-A2	0.56 / 0.80 / 1.10	1.03 / 1.48 / 2.08	2.06 / 3.00 / 4.29
SRES-B1	0.49 / 0.70 / 0.98	0.76 / 1.11 / 1.57	1.17 / 1.74 / 2.57

SRES-B2	0.53 / 0.75 / 1.05	0.84 / 1.22 / 1.73	1.33 / 1.97 / 2.88
SUM	**0.49** / **0.78** / **1.17**	**0.76** / **1.35** / **2.08**	**1.17** / **2.09** / **4.29**

2.3 Scenarios derived from the daily values by the Delta approach

Apart from the scenarios derived using the pattern scaling method, the scenarios derived from daily GCM outputs were used. In addition to the climatic characteristics involved in the scenarios derived from the monthly data, these scenarios include also changes in daily variability. The scenarios were derived by comparing the statistics (means or standard deviations) derived for the future (2081-2100) vs. present (1961-90) periods. The scenarios for Prague are shown in figure 2.3, sampling errors estimated from the multiple simulations with stochastic weather generator are included.

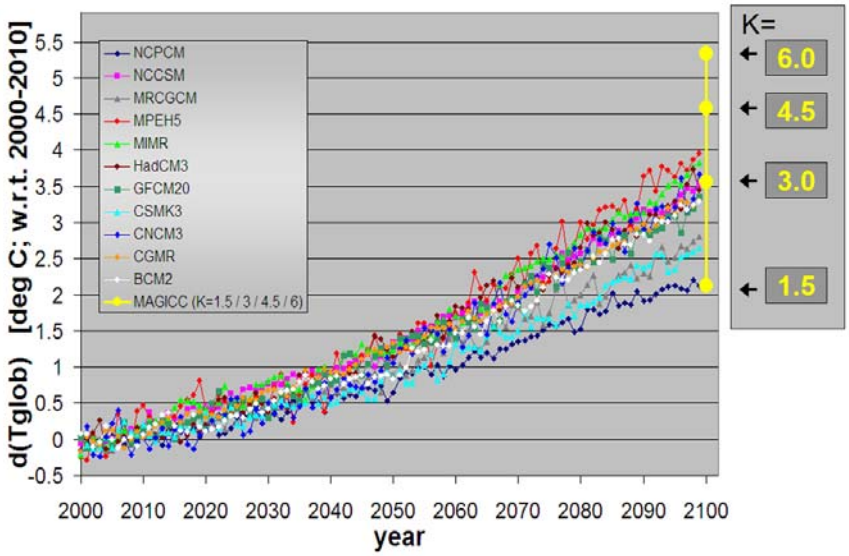

Fig.2.1 Increase of the global mean temperature according to 11 GCMs run under SRES-A2 scenarios and estimate of ΔT_G by MAGICC model (yellow dots) for the SRES-A2 emission scenarios and 4 values of the climate sensitivity (K).

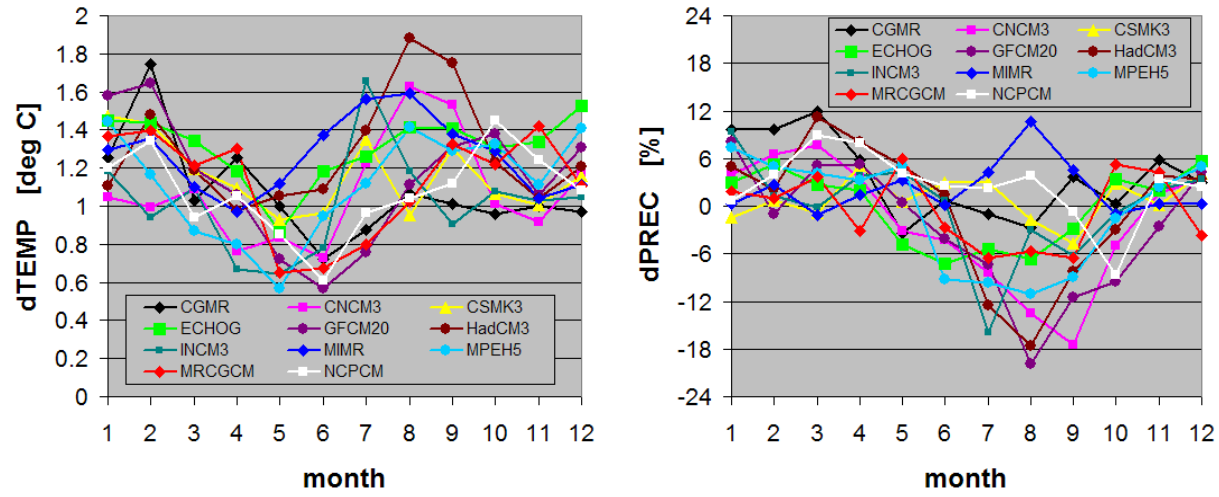

Fig. 2.2 Standardised scenarios of changes in temperature (top) and precipitation (bottom) according to 11 GCMs run under SRES-A2 emission scenario. The changes relate to 1K rise in global mean temperature.

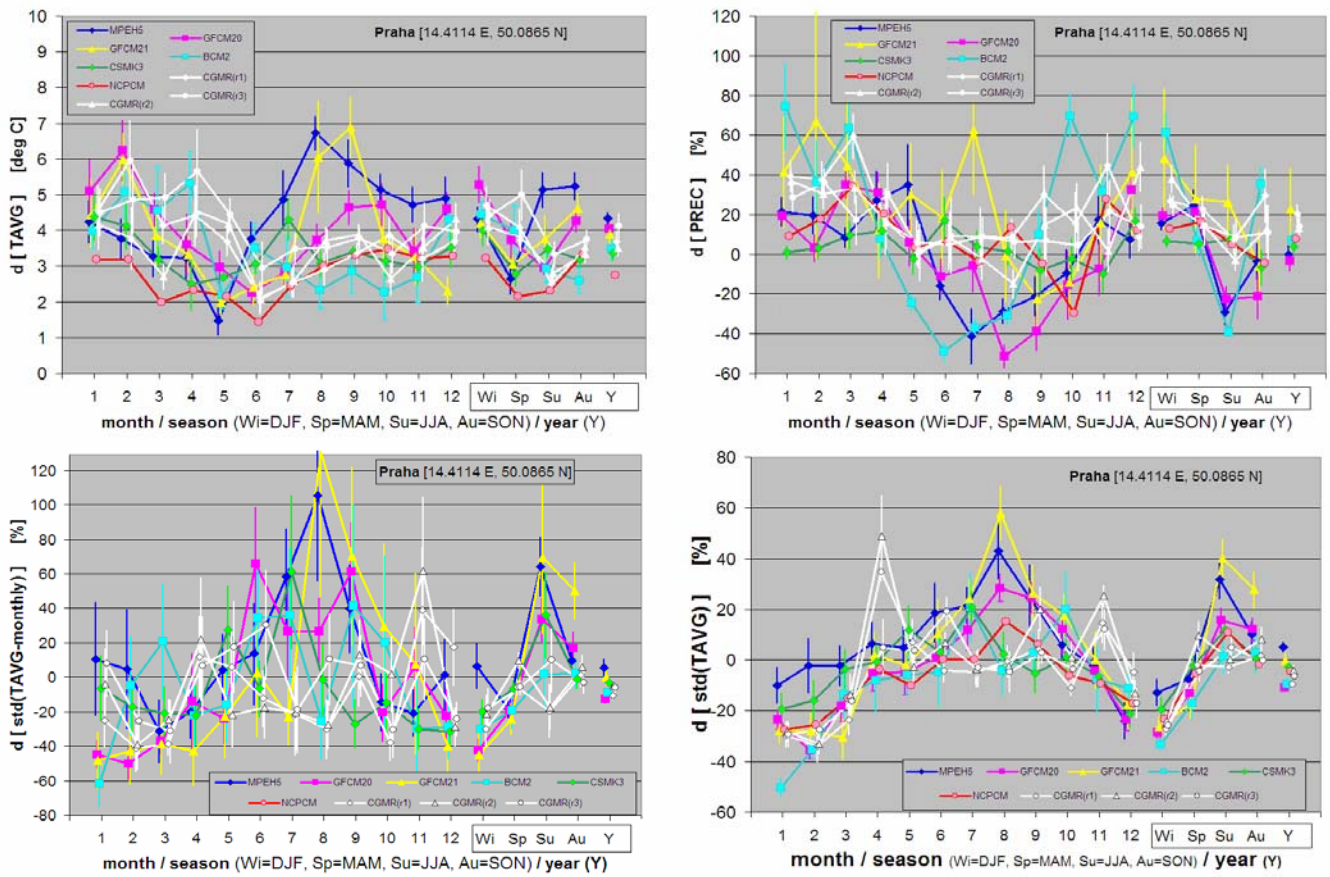

Fig. 2.3 Climate change scenarios derived from the daily outputs of 7 GCMs included in IPCC-AR4 database (3 runs of CGMR are included). Top left: changes in the means of daily average temperature; top right: changes in precipitation sums; bottom left: changes in standard deviation of daily average temperature; bottom right: changes in standard deviation of monthly means of daily average temperature.

References

Dubrovsky M., Zalud Z. and Stastna M., 2000: Sensitivity of CERES-Maize yields to statistical structure of daily weather series. Climatic Change 46, 447- 472.

Dubrovsky M., Buchtele J., Zalud Z., 2004: High-Frequency and Low-Frequency Variability in Stochastic Daily Weather Generator and Its Effect on Agricultural and Hydrologic Modelling. Climatic Change 63 (No.1-2), 145-179.

Dubrovský M., Nemešová I., Kalvová J., 2005: Uncertainties in Climate Change Scenarios for the Czech Republic. Climate Research (v tisku)

Harvey LDD, Gregory J, Hoffert M, Jain A, Lal M, Leemans R, Raper SBC, Wigley TML, de Wolde J (1997) An introduction to simple climate models used in the IPCC Second Assessment Report: IPCC Technical Paper 2 (eds JT Houghton, LG Meira Filho, DJ Griggs, M Noguer), Intergovernmental Panel on Climate Change, Geneva, Switzerland, pp.50

Hulme M, Wigley TML, Barrow EM, Raper SCB, Centella A, Smith S, Chipanshi AC (2000) Using a climate scenario generator for vulnerability and adaptation assessments: MAGICC and SCENGEN Version 2.4 Workbook. Climatic Research Unit, Norwich, UK, pp.52

3. Contribution of NMA

Data and methods

The statistical downscaling models (SDMs) used by the NMA in the CECILIA project are based on the canonical correlation analysis (CCA) technique (Von Storch et al., 1993, Busuioc et al., 1999, 2006). These models have been developed for the mean temperature (94 stations covering the entire Romania) and precipitation total (16 stations covering a southeastern area, used for the impact studies in CECILIA). In a previous work (Busuioc et al., 2006) has been found that, in case of precipitation, it is difficult to find a single skilful SDM for the entire Romanian area, due to the complex Romanian topography.

The temperature field at 850 mb (T850) has been considered as predictor for temperature while the sea level pressure (SLP), geopotential heights at 500 mb (H500) and specific humidity at 850 mb (separately or in combination) have been tested as predictors for precipitation. The temperature SDMs have been developed over the warm (Mai-October) and cold seasons, respectively, considering the respective monthly anomalies together. For precipitation, the SDMs have been developed for each of the four seasons (DJF, MMA, JJA, SON). It has been found that the SDMs for temperature present a high and stable skill while for precipitation, even if the skill is significant, the magnitude of the observed anomalies is not always very well reproduced. More details about the SDM validation are presented in the deliverable D.3.3.

In order to obtained the scenarios for the period 2070-2099, the skilful SDMs calibrated over the period 1961-1990 have been applied to the GCM outputs from 8 ENSEMBLES GCMs (stream1 simulations) under the A1B emission scenario. The ARPEGE outputs have also been used for the temperature scenarios until now. The GCMs used as inputs in the SDMs are: EGMAM (FUB) 3 runs, ECHAM5 3 runs, BCM2 and INGV. The ensemble mean of the SDM projections have been calculated in order to reduce the uncertainties. The full range of the SDM projections for all GCM inputs is also presented. The results are presented in the following.

Fig. 3.1 shows the ensemble mean of the SDM projections averaged for each season (winter, spring summer and autumn). It can be seen that the highest warming is projected for summer (up to 4 ^{o}C over the southern-soutwestern regions). The lowest values are projected for spring. The patterns for winter, spring and autumn show higher values for northwestern regions. These results were compared to those obtained directly from the ENSEMBLES RCM simulations (see Fig. 3.2, example for winter and summer). The following RCMs were considered: CNRM-ARPEGE, DMI-ARPEGE, DMI-ECHAM5, HadRM3Q0-HadCM3Q0, MPI-REMO-ECHAM5, SMHIRCA-BCM2, SMHIRCA-ECHAM5, KNMI-RACMO2-ECHAM5.

The two signals are similar (the SDM signal is a litle bit lower for the southern regions), showing that the SDM results are robust. Comparing the results obtained for each SDM projection, it has been found that the climate signal is dependent on the driver GCM, same conclusion being obtained for the RCMs. Fig. 3.3 shows the spatial average over Romania of the seasonal mean temperature change derived directly from 6 ENSEMBLES RCMs and indirectly through the SDM driven by 7 GCMs (ECHAM5, run 3 gives an unrealistic T850 change over 2070-2099 and it has not been used for the SDM projection). An example for monthly mean temperature change at the 16 stations using the ARPEGE model as SDM driver is presented in Fig. 3.4.

In case of precipitation, the skilful SDMs for each season , calibrated over the period 1961-1990, have been applied to the SLP changes simulated by the 8 GCMs. The results obtained as ensemble average are presented in Table 3.1, showing that, over the analysed area, under the A1B scenario, the precipitation is projected to decrease during the winter and summer months. For the other two seasons (spring and autumn) no significant changes are expected acording to these projections, except for November and some stations in March. The climate signal is similar for various GCM drivers (see Table 3.2) that gives more robustness to the results, especialy for summer when similar findings are obtained from GCMs and RCMs, acording to the results presented by the IPCC AR4 (IPCC, 2007) as well as ENSEMBLES project (Linden and Mithchel, 2009).

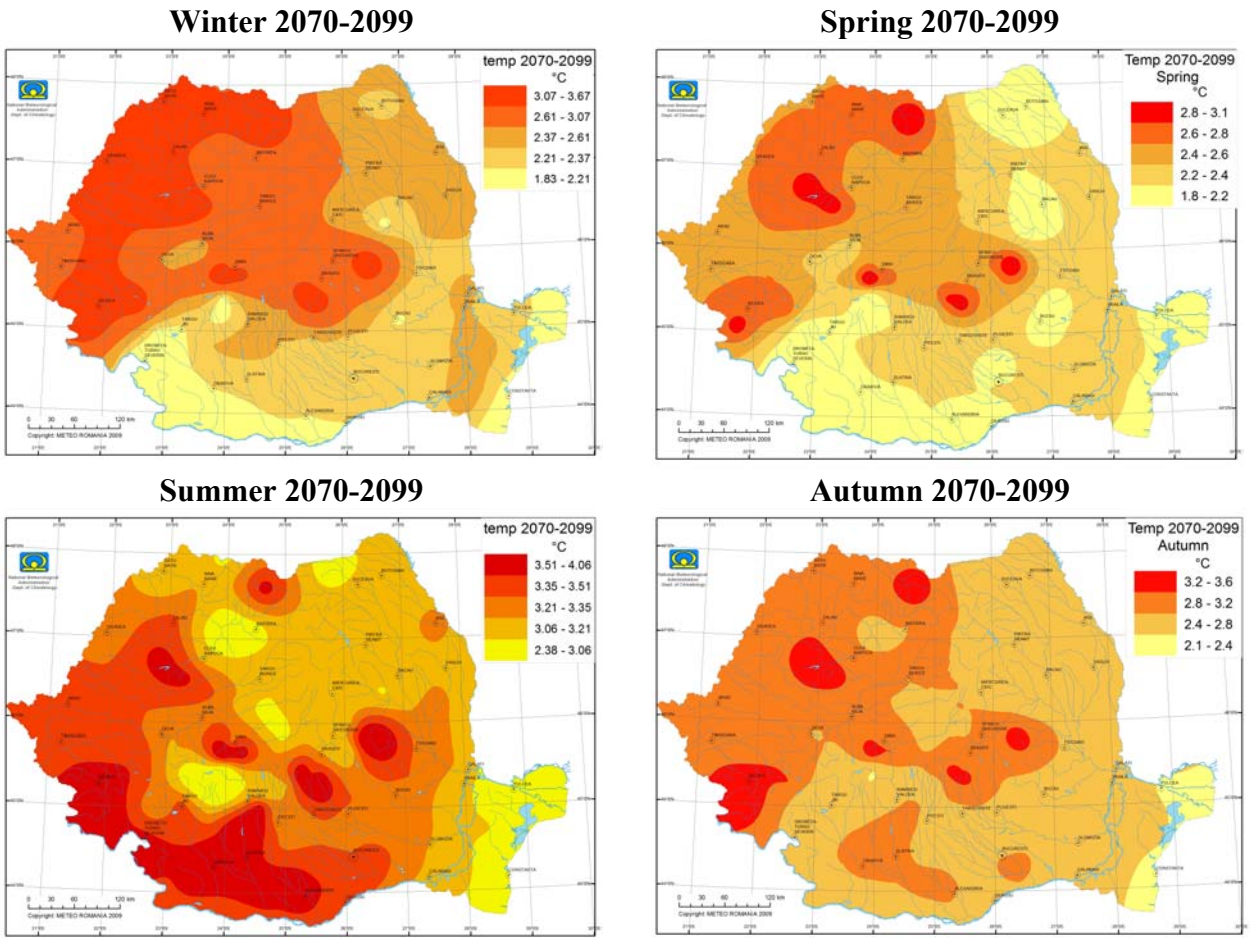

Fig. 3.1. Change of the seasonal temperature mean (2070-2099 vs. 1961-1990) under the A1B emission scenario at 94 stations in Romania (^{o}C) , represented as ensemble mean over SDM projections from the 8 ENSEMBLE GCM simulations (stream 1).

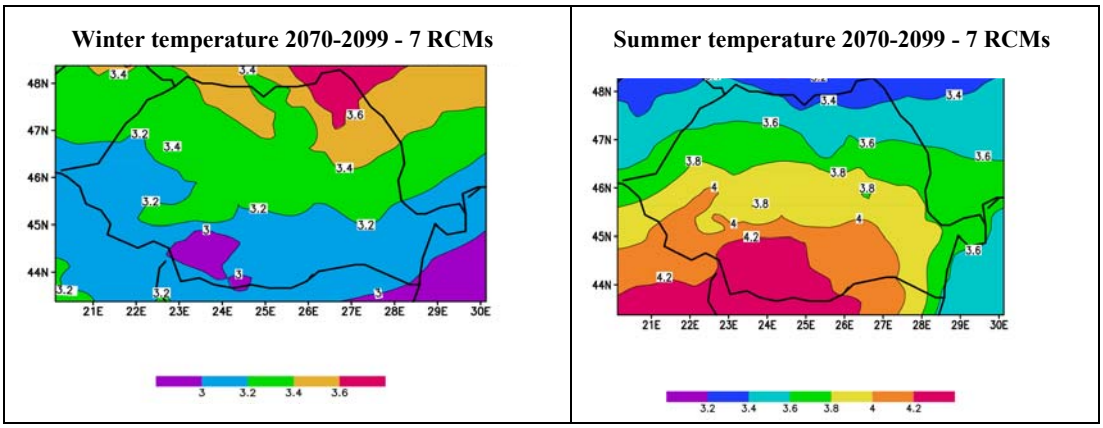

Fig. 3.2. Ensemble mean of winter and summer temperatures changes (2070-2099 vs. 1961-1990) derived directly from 7 ENSEMBLES RCM outputs.

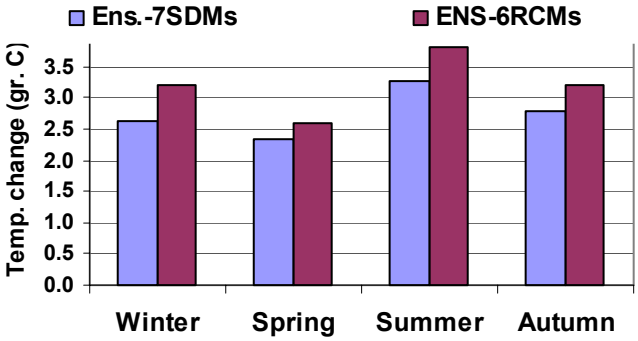

Fig. 3.3. Change of the seasonal mean temperature (2070-2099 vs. 1961-1990), spatial averaged over Romania, derived directly from 6 ENSEMBLES RCMs and indirectly through SDM driven by 7 GCMs.

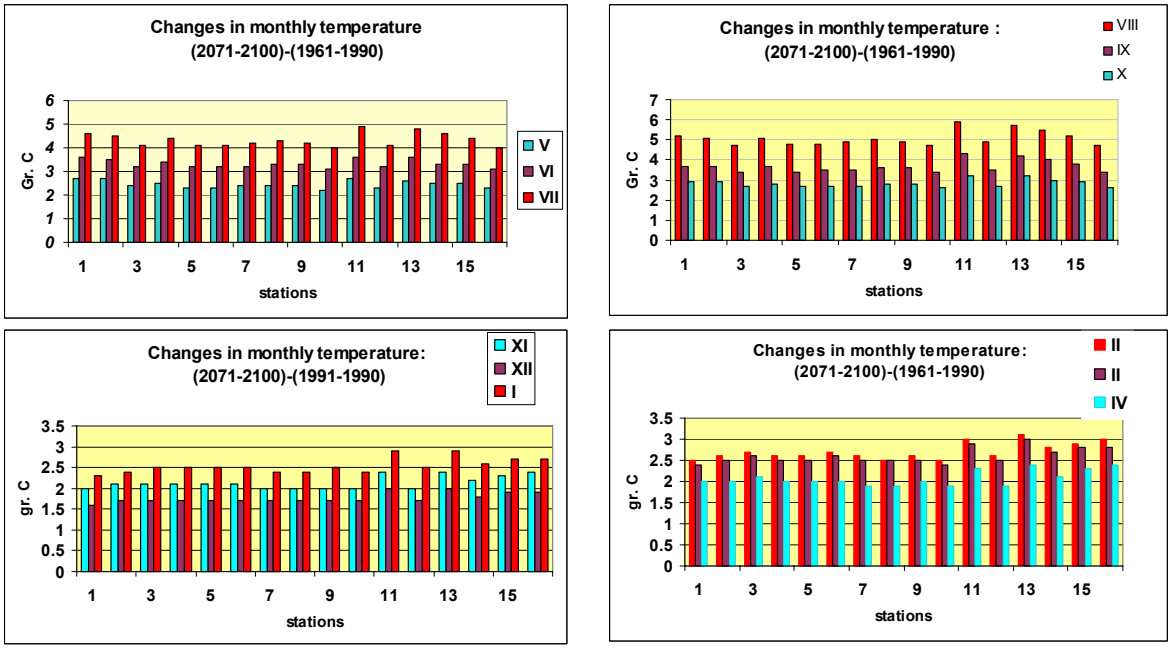

Fig. 3.4. Changes in the monthly mean temperature (2070-2099 vs. 1961-1990) at 16 stations placed in southeastern Romania (see Figure 1 From D3.3) derived from the SDM applied to the T850 anomalies simulated by the ARPEGE GCM under A1B scenario

Table 3.1. Change of the monthly precipitation (%) at 16 stations from the southeastern Romania derived as ensemble average over SDM projections from 8 ENSEMBLE GCM: 2070-2099 vs. 1961-1990, A1B scenario.

Station	Winter			Spring			Summer			Autumn		
	XII	I	II	III	IV	V	VI	VII	VIII	IX	X	XI
Câmpina	-29	-26	-28	-15	-5	1	-8	-5	-6	-4	-1	-20
Călăraşi	-17	-18	-23	-6	-1	1	-19	-23	-22	-1	3	-25
Fundata	-14	-16	-19	-4	1	2	-8	-2	-4	-5	-2	-25
Fundulea	-22	-21	-25	-11	-4	1	-23	-22	-24	1	4	-26
Giurgiu	-22	-20	-24	-8	-2	1	-16	-13	-11	-1	5	-24
Griviţa	-21	-21	-25	-12	-4	1	-20	-20	-18	-2	2	-30
Int. Buzăului	-11	-14	-18	3	4	2	-13	-9	-14	-3	-1	-37
Piteşti	-23	-22	-25	-16	-5	1	-14	-10	-13	-5	1	-23
Ploieşti	-27	-24	-28	-16	-5	1	-10	-8	-9	-1	1	-22
Predeal	-15	-16	-20	-2	2	2	-12	-9	-14	-5	-2	-28
Rm. Sărat	-28	-22	-26	-11	-4	1	-15	-13	-18	-3	1	-25
Sinaia	-25	-21	-23	-13	-4	1	-6	0	-1	-6	-2	-19
Târgovişte	-26	-23	-26	-16	-5	1	-14	-12	-15	-4	1	-24
Tr. Măgurele	-21	-20	-23	-8	-1	1	-13	-6	-1	-1	4	-21
Urziceni	-22	-21	-24	-19	-8	1	-21	-23	-21	0	3	-29
Vf. Omu	-9	-17	-20	12	11	5	-10	-4	-2	1	-2	-30

Table 3.2. Spatial average (over the 16 stations presented in Table 1) of the monthly precipitation change (%) derived from the SDM projections driven by various ENSEMBLE GCMs (stream 1): 2070-2099 vs. 1961-1990, A1B scenario.

Model	Winter			Spring			Summer			Autumn		
	XII	I	II	III	IV	V	VI	VII	VIII	IX	X	XI
BCM2	-38	-8	-55	18	6	-5	0	-3	9	-11	-25	-42
EH5-1	-15	-49	-25	-33	-5	12	-16	-22	-28	2	-30	-27
EH5-2	1	1	1	17	-22	-1	-17	-16	-15	-8	-14	-23
EH5-3	-8	-14	-5	-23	-8	-12	-35	-19	-16	37	24	-13
FUB-1	-34	-11	-29	-25	6	9	0	-3	13	-4	21	-38
FUB-2	-23	-34	-33	-7	-6	18	-5	-6	-31	-29	21	13
Fub-3	-20	-16	-40	-11	10	-4	-33	-25	-27	-2	-3	-51
INGV	-29	-29	-3	-7	5	-6	-4	4	-2	-5	12	-22

References

Busuioc A, von Storch H, Schnur R (1999) Verification of GCM generated regional seasonal precipitation for current climate and of statistical downscaling estimates under changing climate conditions. J Climate 12**:** 258-272.

Busuioc, A, F. Giorgi, X. Bi and M. Ionita, 2006: Comparison of regional climate model and statistical downscaling simulations of different winter precipitation change scenarios over Romania. Theor. Appl. Climatol.,86, 101-124. von Storch H, Zorita E, Cubasch U (1993) Downscaling of global climate change estimates to regional scale: An application to Iberian rainfall in wintertime. J Climate 6: 1161-1171

von Storch H, Zorita E, Cubasch U (1993) Downscaling of global climate change estimates to regional scale: An application to Iberian rainfall in wintertime. J Climate 6: 1161-1171

van der Linden P., and J.F.B. Mitchel (eds.) 2009: ENSEMBLES: Climate Change and its Impacts: Summary of research and results from the ENSEMBLES project. Met. Office Hadley Centre, FitzRoy Road, Exeter EX1 3PB, UK. 160pp.

IPCC, 2007: Contribution of Working Group I to the Fourth Assessment Report of the Intergovernmental Panel on Climate Chang**e** Solomon, S., D. Qin, M. Manning, Z. Chen, M. Marquis, K.B. Averyt, M. Tignor and H.L. Miller (eds.). Cambridge University Press, Cambridge, United Kingdom and New York, NY, USA, 996 pp.

4. Contribution of ELU

Introduction

The applied stochastical downscaling method has two key elements. The first element includes large-scale circulation of the atmosphere and the second element represents a linkage between local surface variables and large-scale circulation. The linkage is expressed by a stochastic model using an observational data series. Then, this model may be utilized with GCM outputs characterizing atmospheric circulation (Mearns et al., 1999).

Stochastic downscaling methods are based on the fact that there exists considerable stochastic relationship between the large-scale atmospheric circulation and the meteorological, hydrological (hydrometeorological) variables. This relationship is estimated from observed data and then is used with large-scale circulation available from GCM output. Thus, an estimation can be obtained for local meteorological and hydrometeorological parameters under a new warmer climate. (Bogárdi et al., 1993). The model was developed and applied for the Carpathian Basin. Computations were carried out using ECHAM driven RegCM regional climate model outputs (25 km horizontal resolution).

Evaluation of precipitation is a much more complicated task than temperature since it has a spatial-temporal intermittence (Bartholy et al., 1995). Therefore, it is necessary to analyze both the probability of precipitation occurrence and its magnitude in wet periods.

Stochastical downscaling methodology in the frame of CECILIA project

First, the stochastic downscaling technique was applied using the ERA-40 datasets for the period 1961-1990. As it is mentioned above, the method is based on the fact that there exists considerable stochastic relationship between the large-scale atmospheric circulation and the meteorological variables (e.g., temperature and precipitation). This relationship was estimated from observed data (i.e., ERA-40 datasets) and then is used with large-scale circulation available from GCM/RCM outputs. Thus, an estimation are obtained for local meteorological parameters under new climate conditions.
Large-scale circulation is characterized by macrocirculation (MCP) types of AT-700 hPa geopotential height data (at 00 UTC) for the region covering the following region with 325 (= 13·25) grid points: 35°-65°N, 30°W-30°E. The MCP types are defined using cluster analysis on a seasonal basis to the corresponding meteorological variables, i.e., temperature or precipitation grid point time series for the region covering Hungary (4·8 = 32 grid points, lat-long: 46°-49°N, 16°-23°E).

Analysis

The statistical downscaling technique was applied for the Carpathian basin using the scenario experiments of RegCM for 3 time slices: 1961-1990, 2021-2050, 2071-2100. AT-700 hPa geopotential height data (at 00 UTC) from the ECHAM-driven RegCM experiments with 25 km horizontal resolution served as the predictor variable for the region covering the previously defined large-scale region. Gridded temperature and precipitation fields for the region covering Hungary (32 grid points, lat-long: 46°-49°N, 16°-23°E) were generated using the downscaling technique, and compared to the results of the RegCM experiments using 10 km horizontal resolution (and using the same 25 km horizontal resolution ECHAM-driven RegCM simulations that provided input fields for the stochastical model).

Results of the 2021-2050 and 2071-2100 periods are presented in D 3.4 and D3.5, respectively.

List of the analyzed parameters:
-- Coded large-scale circulation 40 types (10 types/season)
1. Seasonal averages of cluster centers (AT-700 hPa)
2. Time series of daily codes (1961-1990, 2021-2050, 2071-2100) – seasonal frequency distribution (Fig. 4.1)

-- Temperature
1. Seasonal mean change (Fig. 4.2)
2. Seasonal change of standard deviation (Fig. 4.3)

-- Precipitation
1. Seasonal mean (Fig. 4.4 left panel)
2. Seasonal standard deviation
3. Seasonal mean on wet days only (Fig. 4.4 right panel)
4. Seasonal frequency of wet days (Fig. 4.5)

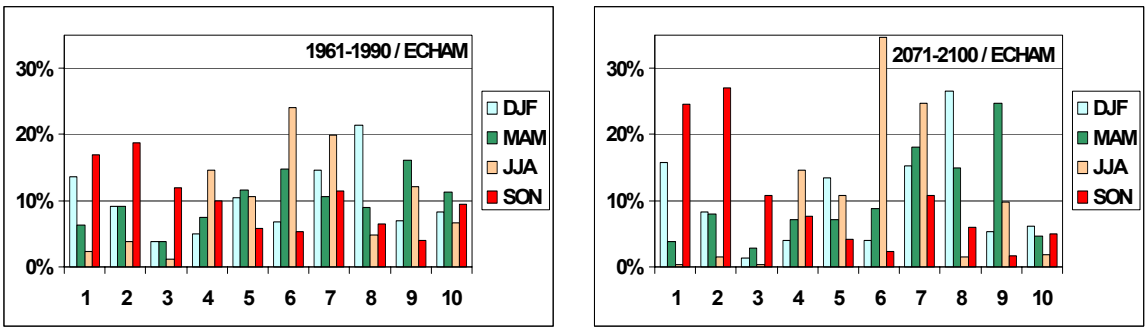

Fig. 4.1: Seasonal distribution of MCP types using the ECHAM-driven simulation fields for 1961-1990 and 2071-2100.

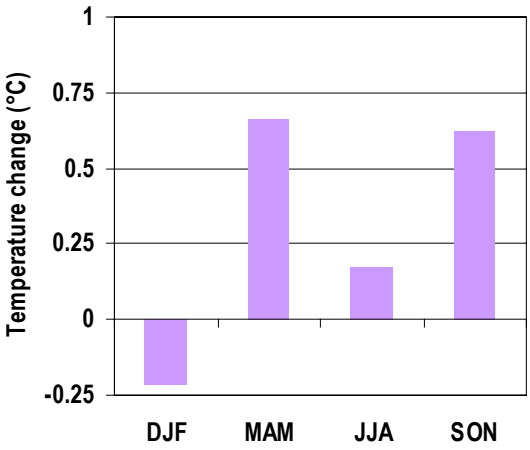

Fig. 4.2: Spatial average of seasonal mean simulated temperature change for Hungary, for 2071-2100 relative to 1961-1990.

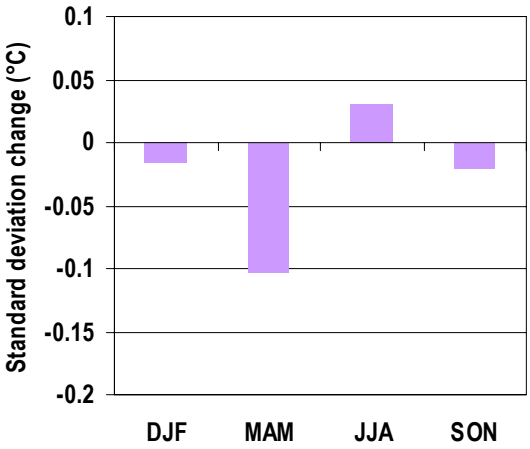

Fig. 4.3: Spatial average of seasonal standard deviation change of simulated temperature for Hungary, for 2071-2100 relative to 1961-1990.

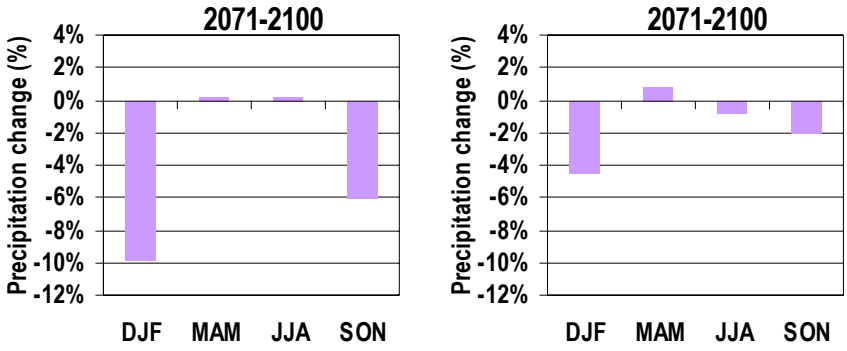

Fig. 4.4: Spatial average of seasonal mean change of simulated precipitation (left panel) and wet-day precipitation (right panel) for Hungary, for 2071-2100 relative to 1961-1990.

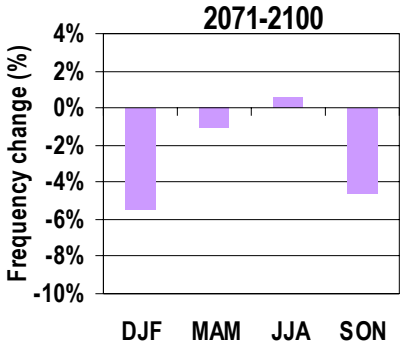

Fig. 4.5: Spatial average of seasonal mean simulated frequency change of precipitation days (R > 1 mm) for Hungary, for 2071-2100 relative to 1961-1990.

Summary of the results of the stochastical-dynamical downscaling model for A1B scenario using RegCM model simulations for Hungary:
(i) Temperature: Seasonal warming is expected between 0.1-0.7 °C, while the spatial average of annual warming is likely to be around +0.3°C.
(ii) Precipitation: In general both the frequency and the amount of precipitation is expected to decrease (by 0-8%).

References

Bartholy, J., Bogárdi, I., Matyasovszky, I., 1995: Effect of climate change on regional precipitation in lake Balaton watershed. Theor. Appl. Climatol. 51, 237-250.

Bogárdi, I., Matyasovszky, I., Bárdossy, A., Duckstein, L., 1993: Application of a space-time stochastic model for daily precipitation using atmospheric circulation patterns. J. Geophys. Res., 98(D9), 16,653-16,667.

Mearns, L.O., Bogárdi, I., Matyasovszky, I., Palecki, M., 1999: Comparison of climate change scenarios generated from regional climate model experiments and empirical downscaling. Special issue on new developments and applications with the NCAR Regional Climate Model (RegCM), J. Geophys. Res., 104(D6), 6603-6621.